Proceeding of the IEEE
International Conference on Robotics and Biomimetics
Dali, China, December 2019

Mechanical Stabilization in Robotic Bionic Eyes with Gravity and Disturbance Compensations[1]

Wei Cheng, Xiaopeng Chen[2], Yang Xu, Xilong Liu[3]

***Abstract*— The vibration of the robot during the movement brings various irregular motion disturbances to the robot's head, these vibration results into unstable images captures by the head-mounted vision system and therefor the vision system cannot accurately perceive the environment. This paper presents a mechanical stabilization method based on gravity and disturbance compensations, which considers and compensates the gravity influences of the mechanical structure and external disturbances. Finally, the current command of the joint motor is generated based on the compensations, which can quickly stabilize the image. We performed simulation and physical experiments to verify the performance of our proposed method.**

***Index Terms*— mechanical stabilization; gravity compensation; disturbance compensation; robotic bionic eyes**

I. Introduction

The vision system (usually in the form of a bionic eyes) mounted on the robot's head is used widely in robot tracking, navigation and mission operations. Since the vibration of the robot during the movement brings various irregular motion disturbances to the head, the mechanical stabilization as one of the stabilization techniques [1] is intended to reduce or even eliminate such disturbance, thus resulting in a good image sequence for the vision system.

Farkhatdinov et al. [2] first proposed the advantages of locating an IMU in the head of a humanoid robot, and used it to mimic the human vestibular system to help improve head stabilization. In another paper [3], it is also mentioned that some researchers achieved head stabilization locating IMU in the KOBIAN robot [4], the WABIAN robot [5] and ROMEO robot [6]. The work of Santos et al. [7] and Oliveira et al. [8] focused on a controller, which combined with genetic algorithm minimized the movement of the head caused by motion. Marcinkiewicz et al. [9] proposed a controller based on the machine learning algorithm that can be quickly learned to compensate for head movements that appear when no stabilization mechanism is present. Yamada et al. [10] and Qiao et al. [11] respectively proposed a head stability model based on continuous model and discrete kinematics, and implemented on the robot. A controller designed by Falotico et al. [12] that uses feedback actual absolute RPY angles of the head and it can follow a reference orientation spanning in the whole workspace of the head and reject the disturbance caused by trunk motion. Inspired by the neuroscientific cerebellar theories, Vannucci et al. [13] presented the first complete model of gaze stabilization, which provided with learning and adaptation capabilities based on internal models. Falotico et al. [14] presented the implementation of three controllers for head stabilization on a humanoid robot. They developed two classic robotic controllers (an inverse kinematics based controller [4][15] and an inverse kinematics differential controller) and a bio-inspired adaptive controller based on feedback error learning [5] and tested on iCub head and SABIAN biped humanoid. However, these methods directly give the joint motor speed command, and there is a certain delay in the system control loop. In design of the robot's head, the eccentric structure is very common. But to the best of my knowledge the influence of gravity is not considered and compensation measures are not taken in their methods. Various machine learning algorithms are employed in most methods, resulting in a complicated system and limited use scenarios.

In this paper, we proposed a mechanical stabilization method based on gravity compensation and disturbance compensation. First, considering that the robot head is almost all eccentric structure, we use the gravity compensation method to reduce the gravity influence of the mechanical structure. Then, the disturbance compensation method is used to weaken the influence of various irregular disturbances during the robot motion. Finally, the current command of the neck joint motor is directly generated to ensure the rapid response of the system control loop.

II. Method

The proposed mechanical stabilization method is characterized by an error-based feedback control that combines gravity compensation and disturbance compensation. Since the design of the robot's head is mostly an eccentric structure, it is extremely effective to compensate for the deviation due to gravity for controlling motion of the motor. Also, in the case of disturbance, to improve the performance of disturbance suppression, we should give

[1]This work was supported by the Science and Technology Program of Beijing Municipal Science and Technology Commission (Z191100008019004).

[2]Xiaopeng Chen is this paper's corresponding author, he is with the school of Mechatronical Engineering, Beijing Institute of Technology, and the key Laboratory of Biomimetic Robots and Systems, Ministry of Education xpchen@bit.edu.cn

[3]Xilong Liu is with the Institute of Automation, Chinese Academy of Sciences, Beijing, 100190, China (email: xilong.liu@ia.ac.cn).

978-1-7281-6321-5/19//$31.00 ©2019 IEEE

priority to the disturbance of system output [16]. Therefore, after being subjected to speed disturbance, the command transmitted to the speed controller should be the position controller output plus the disturbance speed command, otherwise, there will always be disturbance effects and good control effects cannot be obtained.

The 7-DOF bionic eyes vision platform as shown in Fig. 1 is designed with 3 DOFs in the neck and 2 DOFs in each eyeball. The neck has three joints connected in series, while the range of yaw, roll and pitch angles can be up to $\pm 80°$, $\pm 40°$ and $-15° \sim +55°$. The left and right eyeballs are symmetrical, and the range of their yaw and pitch can be up to $\pm 55°$ and $-65° \sim +90°$. Due to the ingenious structural design, the maximum speed of all bionic eye's joints can reach 10 rad/s, which can imitate some movements of a human head to a high degree.

Fig. 1. Bionic Eyes Vision Platform

A. Gravity Compensation

We recorded the yaw, roll and pitch of our bionic eyes neck as joint 1, joint 2 and joint 3 respectively. These frames of reference are considered for our bionic eye's model: (1) the world reference frame $Oxyz$; (2) three neck reference frames of the bionic eyes. We use $\boldsymbol{A}$ to represent the transformation matrix between reference frames, $\boldsymbol{R}$ to represent the rotation matrix between reference frames, $\boldsymbol{g}$ to represent the gravitational acceleration vector, m to represent the mass of the mechanical structure between the joints, and $\boldsymbol{r}$ to represent the vector from the origin of the reference frame to the centroid of the mechanical structure. Where bold the vector, for example, ${}^{0}\boldsymbol{A}_1$ describes the transformation matrix from the world frame to joint 1 frame, ${}^{0}\boldsymbol{R}_1$ describes the orientation of the joint 1 with respect to the world, ${}^{0}\boldsymbol{g}$ represents the gravitational acceleration vector in the world frame. The mass of the mechanical component between the second joint and the third joint is m_2, and the origin of the frame of joint 2 to its centroid is represented as ${}^{2}\boldsymbol{r}_2$. It can be seen in the Fig. 2.

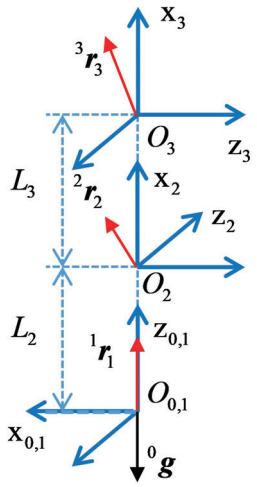

Fig. 2. D-H Model of Bionic Eye's Neck

In the model, the rotation matrix ${}^{0}\boldsymbol{R}_i$ of the world reference frame and the IMU reference frame can be obtained by the IMU's posture angle $(\varphi, \vartheta, \psi)$:

$$ {}^{0}\boldsymbol{R}_i(\varphi, \vartheta, \psi) = \boldsymbol{R}_z(\varphi)\, \boldsymbol{R}_y(\vartheta)\, \boldsymbol{R}_x(\psi) \tag{1} $$

where $\boldsymbol{R_z}$, $\boldsymbol{R_y}$, and $\boldsymbol{R_x}$ represent rotation matrices that rotate around the z, y and x axes, respectively.

For the third joint, the torque is calculated as follows:

$$ T_1 = \left({}^{3}\boldsymbol{r}_3 \times m_3\, {}^{3}\boldsymbol{R}_i\, {}^{i}\boldsymbol{R}_0\, {}^{0}\boldsymbol{g} \right) \cdot \boldsymbol{z} \tag{2} $$

where $\boldsymbol{z} = [0, 0, 1]^T$, ${}^{0}\boldsymbol{g} = [0, 0, g]^T$, and g is the local gravity acceleration value.

For the second joint, the torque is collectively effected by two parts, thus:

$$ \begin{aligned} T_2 = &\left({}^{2}\boldsymbol{r}_2 \times m_2\, {}^{2}\boldsymbol{R}_i\, {}^{i}\boldsymbol{R}_0\, {}^{0}\boldsymbol{g} \right) \cdot \boldsymbol{z} \\ &+ \left({}^{2}\boldsymbol{A}_3\, {}^{3}\boldsymbol{r}_3 \times m_3\, {}^{2}\boldsymbol{R}_i\, {}^{i}\boldsymbol{R}_0\, {}^{0}\boldsymbol{g} \right) \cdot \boldsymbol{z} \end{aligned} \tag{3} $$

Similarly, the torque of the first joint calculated as follows:

$$ \begin{aligned} T_3 = &\left({}^{1}\boldsymbol{r}_1 \times m_1\, {}^{1}\boldsymbol{R}_i\, {}^{i}\boldsymbol{R}_0\, {}^{0}\boldsymbol{g} \right) \cdot \boldsymbol{z} \\ &+ \left({}^{1}\boldsymbol{A}_2\, {}^{2}\boldsymbol{r}_2 \times m_2\, {}^{1}\boldsymbol{R}_i\, {}^{i}\boldsymbol{R}_0\, {}^{0}\boldsymbol{g} \right) \cdot \boldsymbol{z} \\ &+ \left({}^{1}\boldsymbol{A}_3\, {}^{3}\boldsymbol{r}_3 \times m_3\, {}^{1}\boldsymbol{R}_i\, {}^{i}\boldsymbol{R}_0\, {}^{0}\boldsymbol{g} \right) \cdot \boldsymbol{z} \end{aligned} \tag{4} $$

For the gravity compensation of a joint, it is finally reflected in the current command, that is, a preset current command value for the motor of the joint. According to the torque constant:

$$I_{offset} = T/K_I \tag{5}$$

where K_I is the torque constant and is given by the motor.

B. Disturbance Compensation

Since the gyroscope is more sensitive to the speed than joint motor, therefore for the disturbance speed we get the following relationship:

$$\omega_d = \omega_g - \omega_m \tag{6}$$

where ω_d is the disturbance speed, ω_g is the gyroscope speed, and ω_m is the motor speed.

Three joints of our bionic eye's neck are completely orthogonal. When we assemble the gyroscope, we only need to align the three axes of the gyroscope with the three joint axes of the bionic eye's neck. The corresponding three sets of speed quantities are directly obtained, so that complicated kinematics calculation is not required.

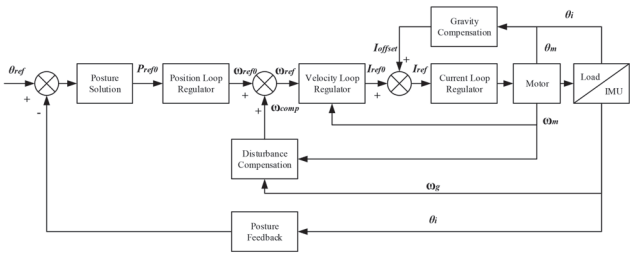

Fig. 3. Control Model

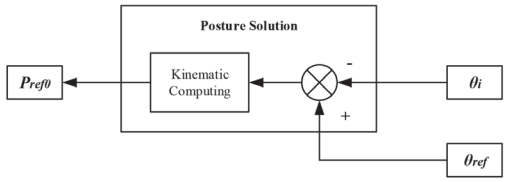

Fig. 4. Posture Solution Model

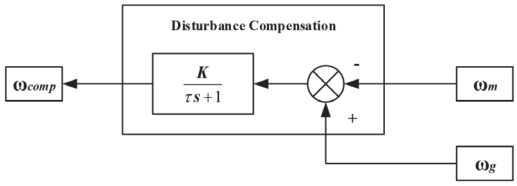

Fig. 5. Disturbance Compensation Model

C. Control Model

The system structure of our mechanical stabilization can be represented by Fig. 3, and the posture solution model shown as Fig. 4. Where θ_i represents the posture angle of the IMU, θ_m represents the angle of rotation of the motor, and P_{ref0} represents the reference value of the position of the joint motor after the posture solution. According to the set IMU's desired posture and real-time feedback value, the command value of the position loop controller is obtained. Then, the command value of the speed loop controller is obtained by the disturbance compensation. Next, the command value of the current loop controller is obtained by gravity compensation. Finally, the current command of the joint motor is obtained.

Based on the previous work [17], we developed a new disturbance compensation link as shown in Fig. 5. Both the speed ω_m of the motor and the speed ω_g of the gyroscope are measurable and together serve as inputs for disturbance compensation. However, due to the presence of measurement noise, we adopt the first order inertial link filter $\frac{K}{\tau s+1}$ to do smoothing, while τ is the time constant of it. We also add a gain K to that link, which is a constant coefficient in the range $[0, 1]$. When $K = 0$, the compensation is completely canceled, and when $K = 1$, the complete compensation is achieved. K can be adjusted based on the experience, and the selection of its value is related to the system: when the external disturbance velocity is higher than the motor itself or the external disturbance has obvious disturbance to the system, then the weight is selected relatively large, and the value of K is close to 1. When the external disturbances are lower than one order of magnitude below compared with the motor feedback speed, the K value can be taken relatively small, such as 0.1; the specific K value is adjusted according to the actual effect.

III. Results and Discussion

To verify the method we proposed, we conducted simulation experiments and physical experiments.

In the process of data analysis, we used the variance and the maximum value to evaluate the stability effect. Take some data in steady state and recorded the data as $\theta_i\,(i = 1, 2, 3, ..., k)$, where k is the amount of data taken. The fixed position reference value is recorded as θ, then the standard deviation is calculated as follows:

$$s = \sqrt{\frac{\sum_{i=1}^{k}(\theta_i - \theta)^2}{k}} \tag{7}$$

A. Simulation Experiments

We built a simulation model in MATLAB environment to verify our proposed mechanical stabilization method. To better simulate the actual disturbance, we mixed two sets of

sinusoidal signals with different amplitudes and frequencies as the source of disturbance. While the frequency and magnitude of one set of disturbances were 1 HZ and 60°, and the frequency and amplitude of the other set of disturbances were 5 HZ and 30°, respectively. A step signal with an amplitude of 100° is given as the desired value of the IMU posture. The experiment is divided into two groups, one is the experimental group using the proposed method, and the other is the controlled group without any compensation.

The results of simulation experiments are shown in Fig. 6, in which the black curve represents the given posture command, the red curve represents the real-time IMU posture using our proposed method, and the blue curve is the real-time IMU posture without any compensation.

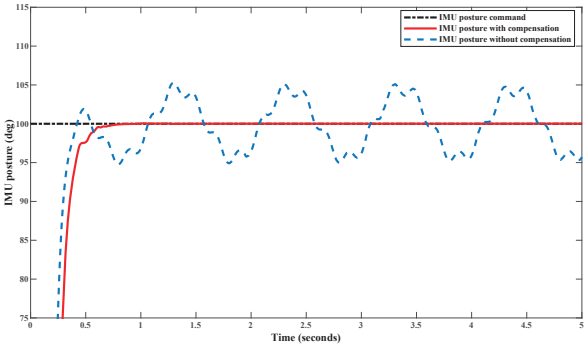

Fig. 6. Simulation Results of Mixed Disturbance

We recorded the experimental data of a steady state, and analyze it. (1) The system without disturbance compensation has a rise time of 0.2218 s, the standard deviation after stabilization is 0.0196, the maximum value is 105.3°, and the minimum value is 94.91°; (2) Adding a disturbance compensation system, the rise time is 0.2557 s, and the standard deviation after stabilization is 7.5876×10^{-5}, the maximum value is 100.1°, and the minimum value is 99.97°.

According to the simulation experiments, it can be seen that after the compensation is added, the system state can be stabilized quickly even after being disturbed, and the lifting effect is obvious compared with the controlled experiment without any compensation.

B. Experiments on 7-DOF Bionic Eyes Vision Platform

We use the six-axis vibration platform as shown in Fig. 7 to provide external disturbance to the 7-DOF bionic eyes vision platform. The vibration platform can realize the three-axis movement and rotation through three sets of steering gears in three-dimensional space. While the range of movement along the x, y and z axis can reach ±38 mm, ±38 mm and ±18 mm, and yaw, roll and pitch angles range can be up to ±20°, ±12° and ±12° respectively.

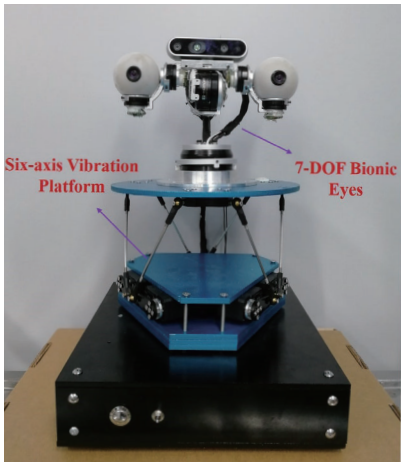

Fig. 7. 7-DOF Bionic Eyes with a Six-axis Vibration Platform.

To verify the compensation effect and rapid response of our proposed method, we performed two sets of experiments on 7-DOF bionic eyes vision platform. Both sets of experiments give a fixed IMU desired posture, but provided disturbance of different frequencies and amplitudes.

1) the First Set of Experiments: In this set of experiments, we set the parameters on the six-axis vibration platform so that the IMU is subjected to a sinusoidal disturbance with a frequency of 0.1 Hz and an amplitude of 8° in the roll, yaw and pitch directions. And the desired angle of IMU roll, yaw and pitch directions set as 0°.

The results are shown in Fig. 8, in each subgraph, the black curve represents the given posture command, the red curve represents the real-time IMU posture using the proposed method, and the blue curve is the real-time IMU posture without any compensation. The standard deviation of each IMU axis under two methods is shown in Table I. Compared with the controlled experiment without any compensation, the experiment using our proposed method has a better performance of mechanical stabilization, and especially in the pitch direction.

2) the Second Set of Experiments: In this set of experiments, we increased the vibration frequency to 0.2 HZ and did not change other conditions and parameters.

The results are shown in Fig. 9, in each subgraph, the red curve represents the real-time IMU posture using the proposed method, and the blue curve is the real-time IMU posture without any compensation. The standard deviation of each IMU axis under two methods is shown in Table I. The yaw and roll direction data still maintain a low standard deviation, and the standard deviation of the yaw direction is still at a large level.

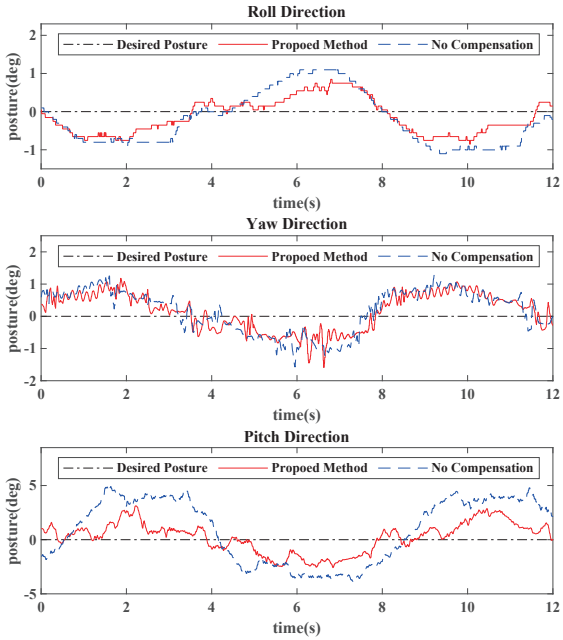

Fig. 8. Results of the proposed method and the method without any compensation after the IMU subjected to a sinusoidal disturbance with a frequency of 0.1 HZ and an amplitude of 8° in the yaw, roll and pitch directions.

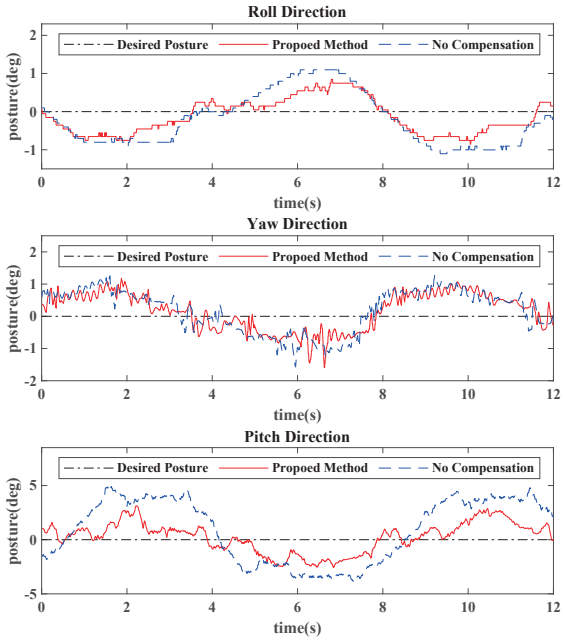

Fig. 9. Results of the proposed method and the method without any compensation after the IMU subjected to a sinusoidal disturbance with a frequency of 0.2 HZ and an amplitude of 8° in the yaw, roll and pitch directions.

TABLE I
THE STANDARD DEVIATION OF EACH IMU AXIS

Number[1]	Method	Yaw	Roll	Pitch
1	Proposed Method	0.606°	0.4843°	1.3507°
	Controlled Method[2]	0.6847°	0.7273°	3.0416°
2	Proposed Method	0.5976°	0.4802°	1.4169°
	Controlled Method[2]	0.69°	0.7187°	3.0595°

[1] The serial number of the two groups of experiments.
[2] The controlled method used mechanical stabilization without any compensation measures.

Through two sets of comparative experiments, we can see that in the direction that is less affected by gravity (yaw and roll direction), our proposed method is less prominent than the method without any compensation, but in the direction that is greatly affected by gravity it has a better performance in both mechanical stabilization and response speed. Because of the design of the 7-DOF bionic eyes platform, the gravity influence of yaw, roll and pitch joints is from small to large. Especially in pitch joint, using a structural design similar to the inverted pendulum, the effects of gravity are more prominent. Our experimental results confirm the effectiveness of the proposed method.

IV. CONCLUSION

We proposed a mechanical stabilization method based on gravity compensation and disturbance compensation for robotic bionic eyes. The method considers the influence of the gravity of the mechanical structure and the external disturbance, and compensates them, and finally generates the current command of the neck joint motor to achieve mechanical stabilization.

Experiments show that our method improves the stability of the robot head vision system and achieves better results than the method without gravity compensation and disturbance compensation. The angular deviations of yaw, roll and pitch in steady state are not more than 0.5°, 0.7° and 1.5° respectively. The method we proposed performed well in terms of mechanical stabilization.

REFERENCES

[1] P. Rawat and J. Singhai, "Review of motion estimation and video stabilization techniques for hand held mobile video," *Signal & Image Processing: An International Journal (SIPIJ) Vol*, vol. 2, 2011.

[2] I. Farkhatdinov, V. Hayward, and A. Berthoz, "On the benefits of head stabilization with a view to control balance and locomotion in humanoids," in *2011 11th IEEE-RAS International Conference on Humanoid Robots*. IEEE, 2011, pp. 147–152.

[3] I. Farkhatdinov, H. Michalska, A. Berthoz, and V. Hayward, "Review of anthropomorphic head stabilisation and verticality estimation in robots," in *Biomechanics of Anthropomorphic Systems*. Springer, 2019, pp. 185–209.
[4] P. Kryczka, E. Falotico, K. Hashimoto, H. Lim, A. Takanishi, C. Laschi, P. Dario, and A. Berthoz, "Implementation of a human model for head stabilization on a humanoid platform," in *2012 4th IEEE RAS & EMBS International Conference on Biomedical Robotics and Biomechatronics (BioRob)*. IEEE, 2012, pp. 675–680.
[5] E. Falotico, N. Cauli, K. Hashimoto, P. Kryczka, A. Takanishi, P. Dario, A. Berthoz, and C. Laschi, "Head stabilization based on a feedback error learning in a humanoid robot," in *2012 IEEE RO-MAN: The 21st IEEE International Symposium on Robot and Human Interactive Communication*. IEEE, 2012, pp. 449–454.
[6] N. Pateromichelakis, A. Mazel, M. Hache, T. Koumpogiannis, R. Gelin, B. Maisonnier, and A. Berthoz, "Head-eyes system and gaze analysis of the humanoid robot romeo," in *2014 IEEE/RSJ International Conference on Intelligent Robots and Systems*. IEEE, 2014, pp. 1374–1379.
[7] C. P. Santos, M. Oliveira, A. M. A. Rocha, and L. Costa, "Head motion stabilization during quadruped robot locomotion: Combining dynamical systems and a genetic algorithm," in *2009 IEEE International Conference on Robotics and Automation*. IEEE, 2009, pp. 2294–2299.
[8] M. Oliveira, C. P. Santos, L. Costa, A. Rocha, and M. Ferreira, "Head motion stabilization during quadruped robot locomotion: Combining cpgs and stochastic optimization methods," *International Journal of Natural Computing Research (IJNCR)*, vol. 2, no. 1, pp. 39–62, 2011.
[9] M. Marcinkiewicz, R. Kaushik, I. Labutov, S. Parsons, and T. Raphan, "Learning to stabilize the head of a quadrupedal robot with an artificial vestibular system," in *2009 IEEE International Conference on Robotics and Automation*. IEEE, 2009, pp. 2512–2517.
[10] H. Yamada, M. Mori, and S. Hirose, "Stabilization of the head of an undulating snake-like robot," in *2007 IEEE/RSJ International Conference on Intelligent Robots and Systems*. IEEE, 2007, pp. 3566–3571.
[11] G. Qiao, G. Song, Y. Zhang, J. Zhang, and Y. Li, "Head stabilization control for snake-like robots during lateral undulating locomotion," in *2014 IEEE International Conference on Robotics and Biomimetics (ROBIO 2014)*. IEEE, 2014, pp. 392–397.
[12] E. Falotico, C. Laschi, P. Dario, D. Bernardin, and A. Berthoz, "Using trunk compensation to model head stabilization during locomotion," in *2011 11th IEEE-RAS International Conference on Humanoid Robots*. IEEE, 2011, pp. 440–445.
[13] L. Vannucci, S. Tolu, E. Falotico, P. Dario, H. H. Lund, and C. Laschi, "Adaptive gaze stabilization through cerebellar internal models in a humanoid robot," in *2016 6th IEEE International Conference on Biomedical Robotics and Biomechatronics (BioRob)*. IEEE, 2016, pp. 25–30.
[14] E. Falotico, N. Cauli, P. Kryczka, K. Hashimoto, A. Berthoz, A. Takanishi, P. Dario, and C. Laschi, "Head stabilization in a humanoid robot: models and implementations," *Autonomous Robots*, vol. 41, no. 2, pp. 349–365, 2017.
[15] P. Kryczka, E. Falotico, K. Hashimoto, H.-o. Lim, A. Takanishi, C. Laschi, P. Dario, and A. Berthoz, "A robotic implementation of a bio-inspired head motion stabilization model on a humanoid platform," in *2012 IEEE/RSJ International Conference on Intelligent Robots and Systems*. IEEE, 2012, pp. 2076–2081.
[16] B. B. Alagoz, F. N. Deniz, C. Keles, and N. Tan, "Disturbance rejection performance analyses of closed loop control systems by reference to disturbance ratio," *ISA transactions*, vol. 55, pp. 63–71, 2015.
[17] X. Chen, C. Wang, T. Zhang, C. Hua, S. Fu, and Q. Huang, "Hybrid image stabilization of robotic bionic eyes," in *2018 IEEE International Conference on Robotics and Biomimetics (ROBIO)*. IEEE, 2018, pp. 808–813.